Preferred citation: T. Yamauchi and K. Murakami. Observation of deforming and fracturing processes of paper by use of thermography. In **Products of Papermaking**, *Trans. of the Xth Fund. Res. Symp. Oxford, 1993*, (C.F. Baker, ed.), pp 825–847, FRC, Manchester, 2018. DOI: 10.15376/frc.1993.2.825.

Observation of deforming and fracturing processes of paper by use of thermography

Tatsuo Yamauchi and Koji Murakami
Dept. of Wood Science & Technology
Faculty of Agriculture
Kyoto University
Sakyo-Ku Kyoto
Japan

Abstract

Thermography has been found to be useful for detecting the local variations in temperature of paper sheet under strain. The changes in temperature images during the course of tensile straining could describe the local deforming and fracturing process of paper. A thermal deformation pattern of well formed paper was locally uneven, but uniform wholly throughout the specimen. On the other hand, the deformation pattern of poorly formed paper was uneven in micro and macro scale at the early stage of its plastic deformation region. However, the deformation pattern was fairly uniform through the specimen at the later stage of its plastic deformation.

Introduction

The deforming and fracturing processes of paper during straining are directly related to the mechanical strength of paper, and thus are very important for many of paper's practical uses. A great number of studies relating to the deforming and fracturing processes have been made using various methods (1.2). The thermodynamic examination developed by Ebeling is one of the basic studies (3).

Using a gas-filled micro-calorimeter, he measured the heat coming in and going out of paper under strain, and attributed a slight drop of sample temperature at the initial straining region to Kelvin's thermelastic effect and a temperature rise in plastic deformation region to the irreversible intrafibre deformation. Those explanations ere in accordance with those from recent studies using AE techniques (4.5).

Thermal behaviour of paper under strain has also been studied by using a liquid crystal thermal analysis (6) and a line scanning type of infrared thermal camera (7). The results showed that paper during straining exhibited a fairly uniform distribution of temperature rise.

Recently a new technique of infrared thermography was successfully introduced to observe the local temperature changes of a handsheet under strain suggesting the stress distribution as a temperature distribution image (8,9). In the present paper this technique is employed for studying how the stress concentrates or distributes within a paper specimen under tensile strain and how the pattern of the stress distribution relates to the failure zone and further to the effect of change in paper structure introduced by papermaking conditions such as refining and formation on the stress distribution.

Infrared thermography

Applying the temperature measurement system based on infrared radiation, an infrared thermograph was developed to obtain a thermal image, i.e. map of temperature in the mid 1960s. The principle of this method is as follows: An infrared camera scans a specimen in the horizontal and vertical directions and then displays the surface temperature distribution as a colour image. At first, it was used primarily in the medical field for breast cancer detection. Progress in infrared sensing, which included an improvement of temperature determination sensitivity of $0.1^{o}C$ and high speed determination, provided a wider utilisation of this technique in non-destructive testing for quality control and process monitoring in the industrial production environment (10) In the field of pulp and paper, the technique has been used to detect cross-machine moisture profile on the paper machine (11). Recent introduction of a computer aided image processing technique, such as image subtraction, histogram display and average temperature display, has made thermography more versatile and provided wider usage.

Experimental

Materials

A commercial dry bleached softwood kraft pulp was beaten to various degrees with a PFI mill under standard conditions. Handsheets were made from the pulp with the standard sheet mold.

Instrumentation

The experimental arrangement used here is shown in Fig. 1. The paper specimen, carefully cut to 15mm in width by about 70mm in length, was clamped to an Instron-type testing machine (Shimadzu Autograph AGS-100) with a span distance of 50mm, and was strained at a crosshead speed of 20mm/min.

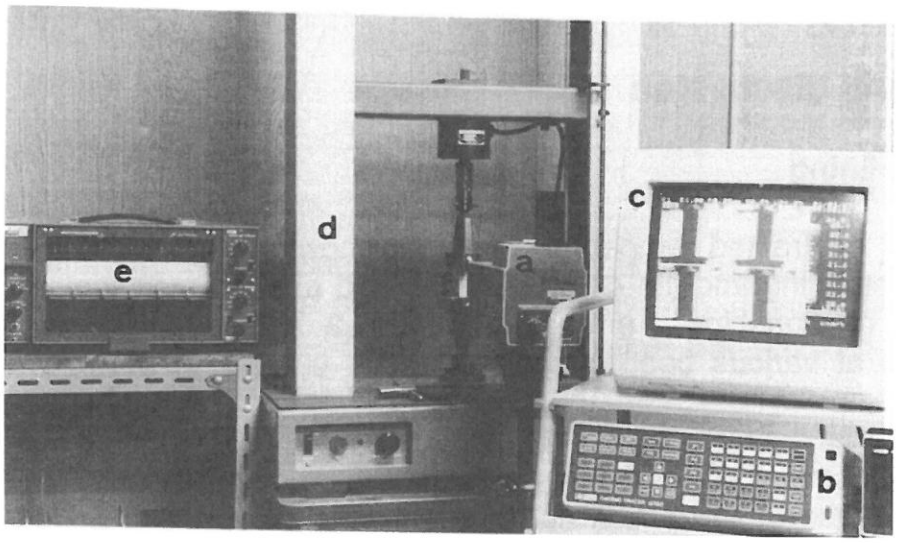

Fig. 1 Setup of infrared thermography for measuring surface temperature of paper under strain ; (a) infrared camera, (b) control unit, (c) monitor display, (d) Instron type machine, (e) recorder, (f) specimen.

The infrared thermal imaging system used here was an Infrared Thermo Tracer 6T62 (NEC San-ei Instruments Ltd). This consists of an infrared camera cooled with liquid nitrogen, a monitoring display and a control unit with image processing function. The camera was positioned on a tripod, about 20cm from the specimen face. The camera contains a HgCdTe dector which is sensitive to infrared radiation in the wavelength range of 8-13μm. It has a temperature difference sensitivity of 0.1°C over a scanned spatial area of about 7x7cm and framing rate of 4 frames per second, and a minimum detectable size of 0.5mm. The temperature imaging data were first recorded on floppy disk and then image processing of the data, such as temperature averaging in a given area and subtracting one temperature image from another temperature image, was carried out.

The displayed temperature was determined using the assumption that the paper sheet was a perfect black body, namely, the emissivity was 1.0.

Due to the high sensitivity of temperature difference in thermography and the complicated thermal environment, the thermograph detects an uneven temperature distribution within the paper specimen even before straining, and displays the distribution in different hues as shown in the previous paper (8). Thus, the change in temperature distribution, which was caused by local deformation and fracturing, was imposed on the initial temperature distribution and made the real change of temperature distribution ambiguous. Therefore, an image subtraction with 1.3% elongation gap was carried out and the subtracted temperature images are examined.

All measurements were carried out in a testing room which was carefully conditioned at 22^{o}C and 65% RH without air circulation.

Results and discussion

Effect of refining

A series of subtracted temperature images showing the deformation process during the straining and the corresponding load and average temperature rise-elongation relationships are shown in Fig. 2 and 3, respectively for the handsheets at various beating degrees. The number in brackets is percent elongation.

After initial cooling due to Kelvin's effect, the average temperature gradually rose with an increase of elongation during the plastic deformation period up to the failure point. The higher the beating degree, the more the average temperature rose. This result suggests that an increase in fibre bonding by beating causes an increase in irreversible fibre deformation. The fairly proportional relationship between average temperature and elongation enables the temperature image to show stress distribution during the straining.

For the handsheet from unbeaten pulp (Fig.2), average temperature rise was not large. A yellow and orange coloured part (showing a slightly higher temperature) locally appeared and a distribution of the high temperature part at every stage of straining was fairly uniform throughout the specimen. Although, a wide distribution of the high temperature part was shown at the upper part of the specimen at the end of the plastic deformation region, in picture (2.3-0.9), at the stage of failure a failure spot (arrow in the picture) has started from the right bottom corner of the specimen and has developed diagonally as shown in pictures (2.4-1.1) and (2.6-1.3).

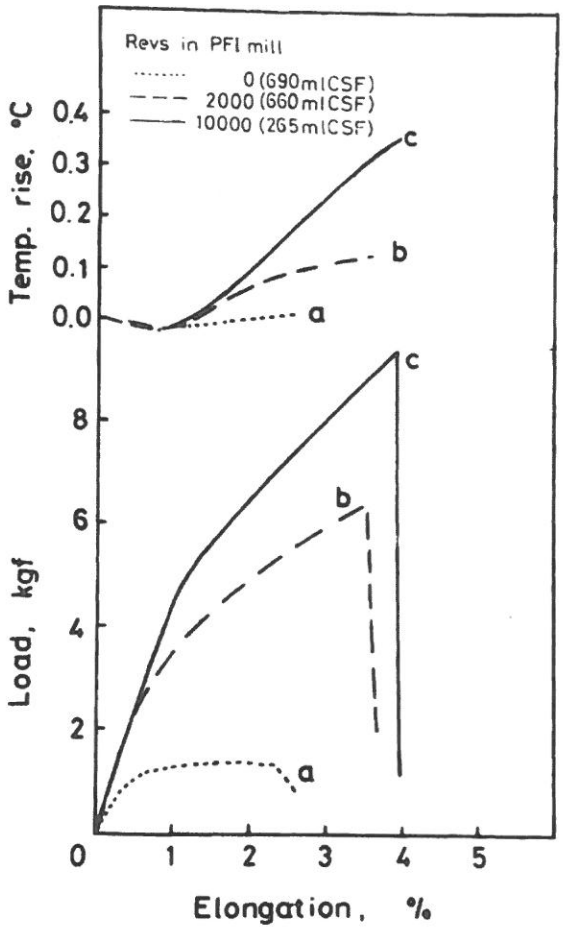

Fig. 3 Load/average temperature rise-elongation relationships for the handsheets from (a) unbeaten pulp, (b) lightly beaten pulp and (c) heavily beaten pulp.

For the handsheet from unbeaten pulp (Fig.2), average temperature rise was not large. A yellow and orange coloured part (showing a slightly higher temperature) locally appeared and a distribution of the high temperature part at every stage of straining was fairly uniform throughout the specimen. Although, a wide distribution of the high temperature part was shown at the upper part of the specimen at the end of the plastic deformation region, in picture (2.3-0.9), at the stage of failure a failure spot (arrow in the picture) has started from the right bottom corner of the specimen and has developed diagonally as shown in pictures (2.4-1.1) and (2.6-1.3).

For the handsheets from lightly (Fig 2b) and heavily beaten pulp (Fig. 2c), the high temperature part was locally uneven, but uniform as a whole throughout the specimen. The distribution of the high temperature part changes at every stage of deformation, and there was no indication of the failure line until the paper sheet started to fail and released the heat derived from mechanical work around the failure line as shown in picture (3.7-2.4) for lightly beaten pulp sheet and picture (4.1-2.8) for heavily beaten pulp sheet.

Effective on additives

We changed fibre bonding ability with two additives, a polyacrylamide resin and a cationic surfactant. The former (bonding agent) is known to increase breaking strength and the later (debonding agent) reduces it.

A series of subtracted temperature images and the corresponding load and average temperature rise - elongation relationships are shown in Fig. 4 and 5 respectively for the handsheets made with the additives and, in comparison, with a control handsheet (CSF 470ml).

Addition of additives caused a slightly poorer formation and some minor changes in sheet density, and a further large change in load-elongation behaviour as shown in Fig. 5.

For the handsheet made with debonding agent (Fig 4a), the high temperature part was distributed on central left side of the specimen from the first picture. The failure spot (arrow) started to develop at the point as shown in picture (1.9-0.6).

For the handsheet made with bonding agent (Fig.4b), the high temperature part was distributed at right side of specimen during the early period of plastic deformation until picture (2.3-0.9) and was uniformly distributed through the specimen at the midway of plastic deformation, and then was distributed at the left side of the specimen at the later period of plastic deformation. Therefore, the distribution of the high temperature part through whole period of plastic deformation was fairly uniform. There was no sign to suggest a final failure spot except for the stage immediately before failure as shown by the arrow in the picture (4.7-3.4).

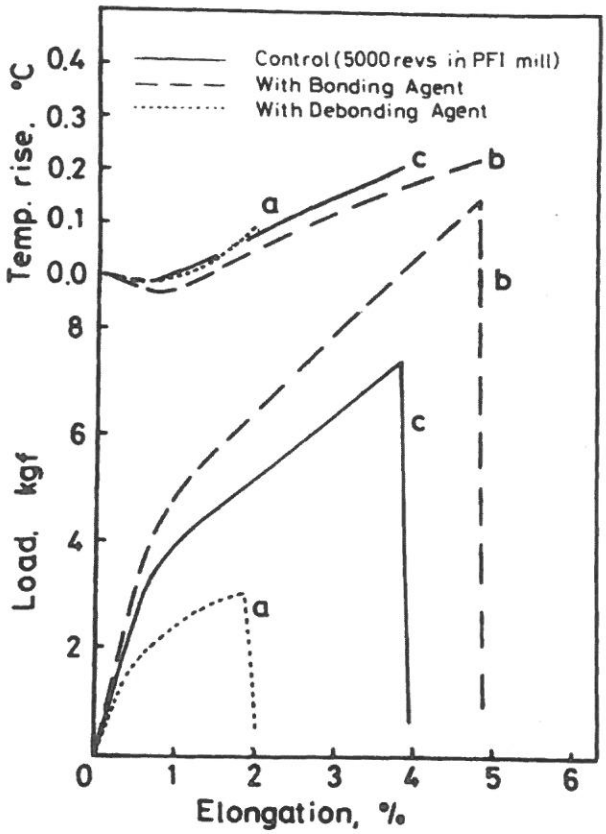

Fig 5. Load/average temperature rise-elongation relationships for the handsheets made with (a) debonding agent, (b) bonding agent and (c) control handsheet.

Effect of formation

When evaluating the effect of sheet formation on the deformation process, two other points i.e. orientation and sheet density also need to be considered (12,13). Therefore, a series of handsheets which were varied in formation conditions, namely, forming stock concentration or settling time in their sheet-making process, were prepared from the same furnish (600ml CSF) to allow for these points.

Table 1 The effect of handsheet forming conditions on tensile strength and elongation.

Forming condition	Tensile strength kgf	Elongation at break
	7.03	4.3
normal [1]	7.02*	3.5*
	7.17	4.5
stock concentration		
	6.80	4.0
2 times (0.034%)	6.41*	3.4*
	6.51	3.3
	5.92	3.4
4 times (0.068%)	6.28*	3.4*
	6.33	3.1
settling time		
	7.20	4.0
30 sec	7.17*	4.3*
	7.08	4.2
	6.14	3.2
100 sec	6.21*	4.0*
	5.86	2.9

(1) stock concentration of 0.017%, settling time of 10 sec
The sequential subtracted temperature images for the test marked in * are shown in Fig.-6

Light transmission and soft x ray images for the 60 g/m^2 handsheets made at normal, two and four times the forming stock concentration and those made with 30 and 100 sec settling time are shown in Fig. 4.

An increase of forming stock concentration or settling time caused poor formation as shown by light transmission and soft x ray images.

For the poorly formed sheet, a remarkably uneven distribution of the high temperature zone appeared at the early stage of plastic deformation. The high temperature zone in the temperature images does not correspond to the low substance part of the sheet which appears as a lighter part in light transmission or soft x ray images. At the later stage of plastic deformation the high temperature contribution is homogeneously distributed throughout the specimen. It is interesting that the final failure line was often placed on one of the high temperature zones at the early stage of plastic deformation. In the case of the sheet made with 30 sec settling time, however, the failure spot was not in the high temperature zone and breaking load is noted to be larger than those of other handsheets.

Currently many commercial papers and paperboards are made by using combination or multilayer forming technology. Consequently, knowledge about effect of interior structure on strength properties becomes very important (14). Figure 7 shows continuous subtracted temperature images during straining for multiply handsheet which was composed with a poorly formed 50 g/m^2 handsheet (bottom side) and a well formed 10 g/m^2 handsheet (top side). The result showed that the deformation of the combined sheet seemed to be governed by that of the main part of the sheet. That is, the high temperature part was unevenly distributed at the first half of the plastic deformation period and evenly distributed throughout the sheet at the second half of the plastic deformation period. Further, the failure line coincided with the high temperature part in the sheet, as shown at the early stage of plastic deformation.

Concluding remarks

Thermal distribution of paper during tensile testing was successfully observed as a colour image by means of an infrared thermography, showing the deforming and fracturing processes of paper.

Temperature distribution of paper having good formation is not uniform in microscale, but uniform in macroscale and further the temperature distribution changes every moment throughout its plastic deformation period up to failure. Therefore, there was no sign to suggest final failure line until the sheet started to fail. On the other hand, temperature distributions of paper having poor formation are not uniform, not only in the microscale, but also in the macroscale at the early stage of plastic deformation. However, they become uniform in macro at the later part of the plastic deformation period. Having a high temperature zone at the early stage of plastic deformation often leads to final failure line.

Acknowledgement

The authors wish to thank Prof. Noguchi for allowing them to use the thermography apparatus and Prof. James L. Davis of the University of Wisconsin-Madison for his critical reading of the manuscript.

References

1 Nordman, L., Gustafsson, C. and Olofsson, G.,'Optical measurement of bond breaking during a tensile test' Tappi J. 38(12):724 (1955)

2 Corte, H., Kallmes, S. and Jarrot, D., ' Mechanical failure of ideal 2-D fibre networks' Paper-Maker 142(7):61 (1961)

3 Ebeling, K., 'Distrubtion of energy comsuption during the straining of paper' Fundamental Properties of Paper Related to its Uses. The 5th Fundamental Reaserch Symposium, Cambridge, UK., 304 (1976)

4 Yamauchi, T., Okumura, S. and Murakami, K., 'Measurement of acoustic emission during the tensile straining of paper' J. Pulp and Paper Sci., 15(1): J23 (1989)

5 Yamauchi, T., Okumar, S. and Noguchi, M., 'Acoustic emission as an aid for investigating the deformation and fracture of paper' J. Pulp and Paper Sci., 16(2): J44 (1990)

6 Lyne, M.B.and Hazell, R., 'Formation testing as a means of montioring strength uniformity' Fundamental Properties of Paper Related to its uses. The 5th Fundamental Research Symposium, Cambridge, Uk., 74 (1976)

7 Dumbleton, D.P., Kringstad, K.P. and Soremark, C., 'Temperature profiles in paper during straining' Svensk Papperstid. 76(14):521 (1983)

8 Yamauchi, T. and Murakami, K., 'Observation of deforming and fracturing processes of paper by using infrared thermography' J. Japan Tappi 46(4):70 (1992)

9 Yamauchi, T., Okumura, S. and Noguchi, M., 'Application of thermography to the deforming process of paper materials' J. Materials Sci., 28 in press (1993)

10 Cielo, P., Maldague, X. Deom, A.A. and Lewak, R., 'Thermographic nondestructive evaluation of industrial materials and structures' Materials Evaluation 45: 452 (1987)

11 Vickerly D.E., Luce, J.E. and Atkins, J.W., 'Infrared thermography, an aid to solving paper machine moisture profile problems' Tappi J. 61(12): 17 (1978)

12 Norman, R.J., 'Dependence of sheet properties on formation and forming variables' Consolidation of the Paper Web. The 3rd Fundamental Research Syposium, Cambridge, UK., 269 (1966)

13 Norman B. and Wahren, D., 'Mass distribution and sheet properties of paper' Fundamental Properties of Paper Related to its uses. The 5th Fundamental Research Syposium, Cambridge, UK., 7 (1976)

14 Hasuike, M., Kawasaki, T and Murakami, K., 'Evaluation method of 3-D geometric structure of paper sheet' J. Pulp and Paper Sci., 18(3) J114 (1992)

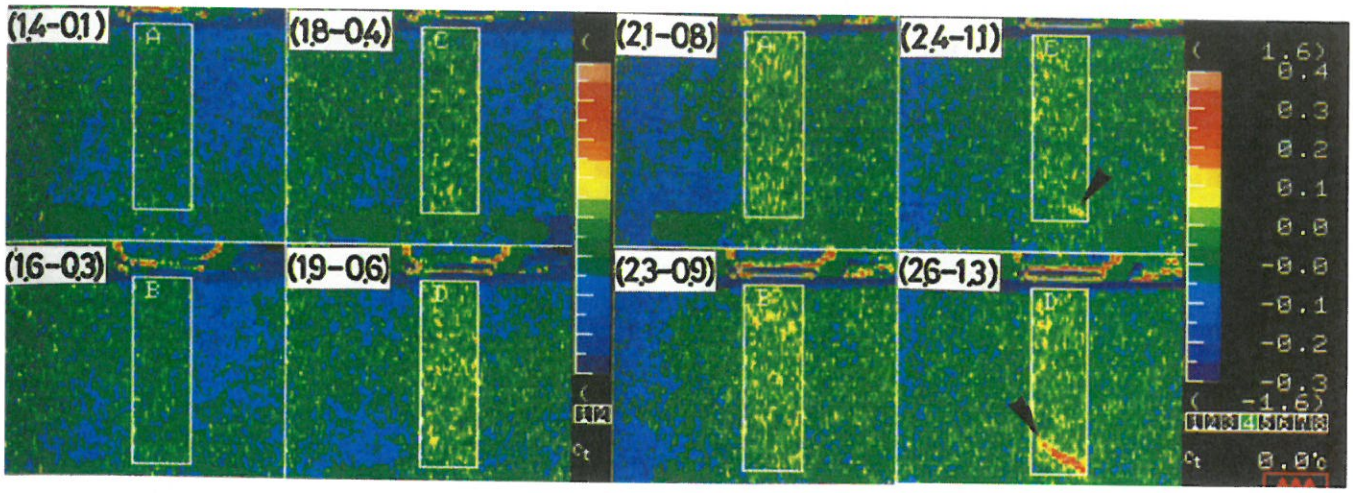

Fig 2a Sequential subtracted temperature images during straining for the handsheet from unbeaten pulp. Number in parentheses is percent elongation

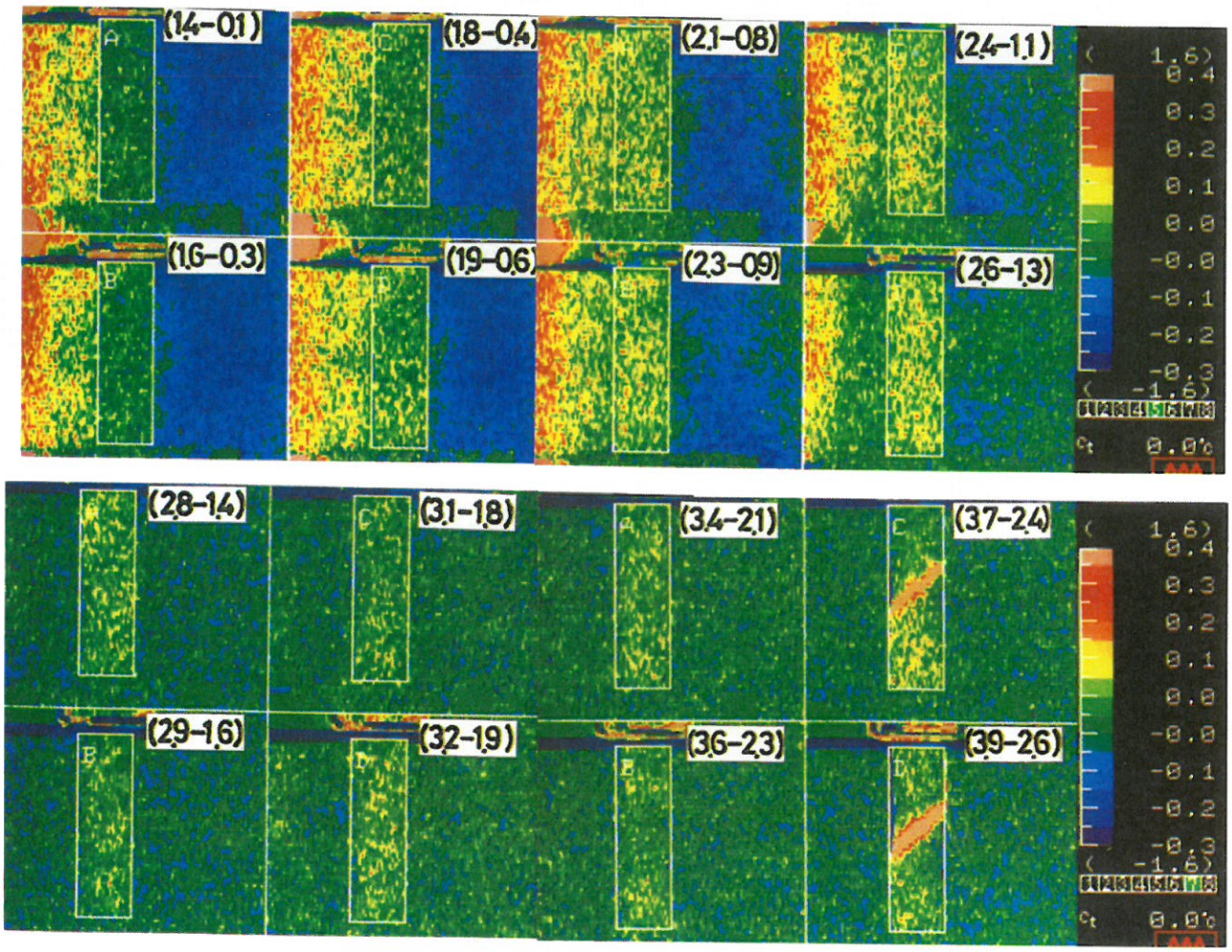

Fig 2b Sequential subtracted temperature images during straining for the handsheet from lightly beaten pulp. Number in parentheses is percent elongation

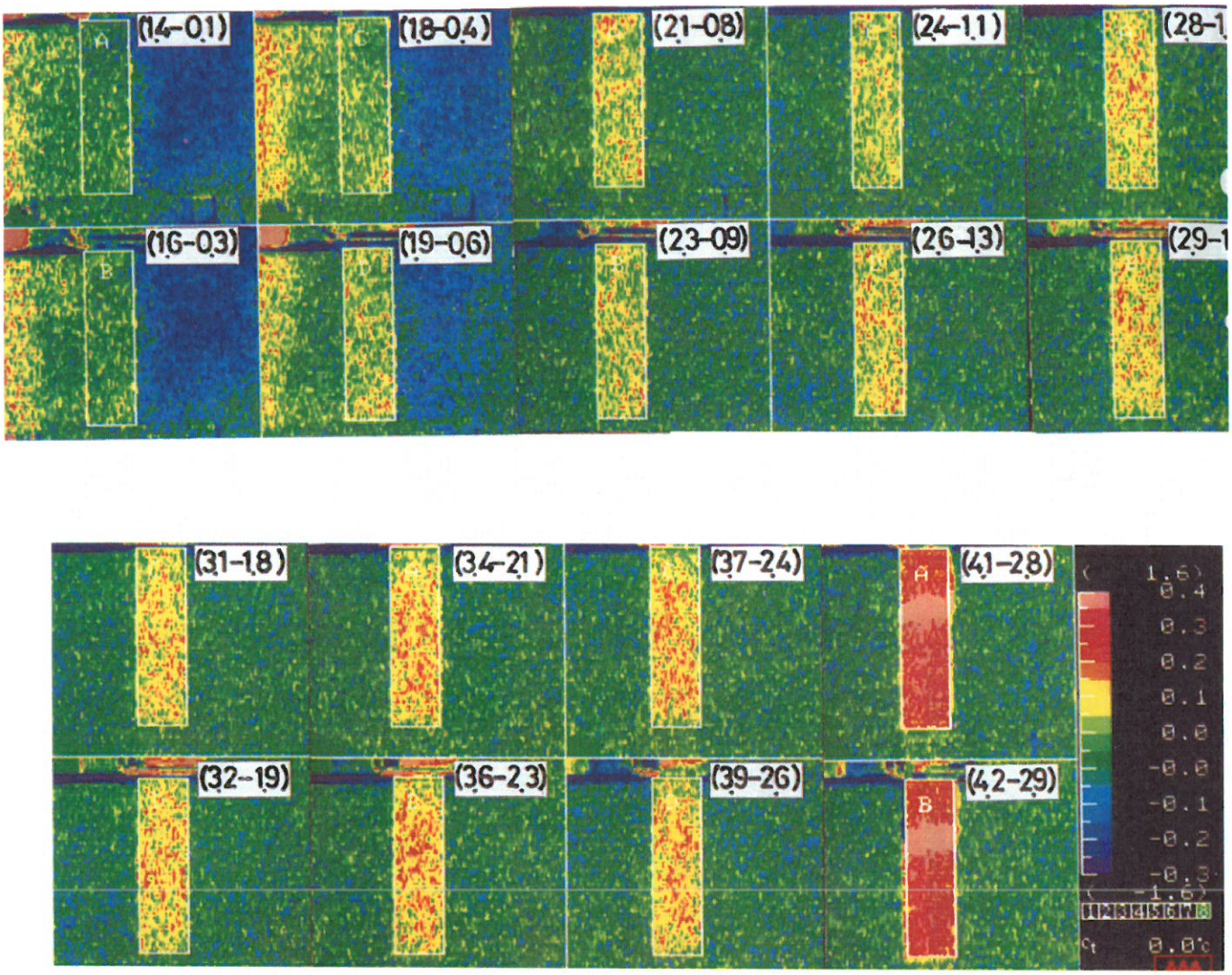

Fig 2c Sequential subtracted temperature images during straining for the handsheet from heavily beaten pulp. Number in parentheses is percent elongation

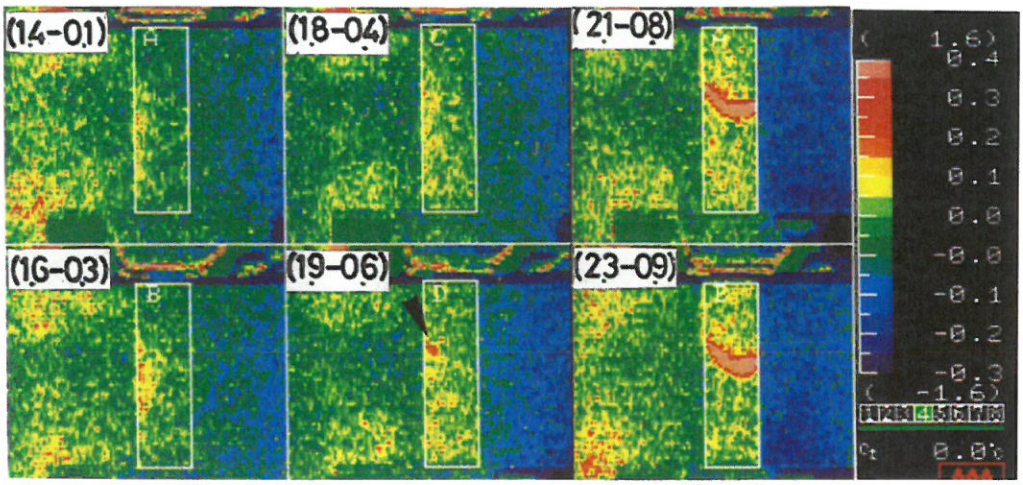

Fig 4a Sequential subtracted temperature images during straining for the handsheet made with debonding agent. Number in parentheses is percent elongation

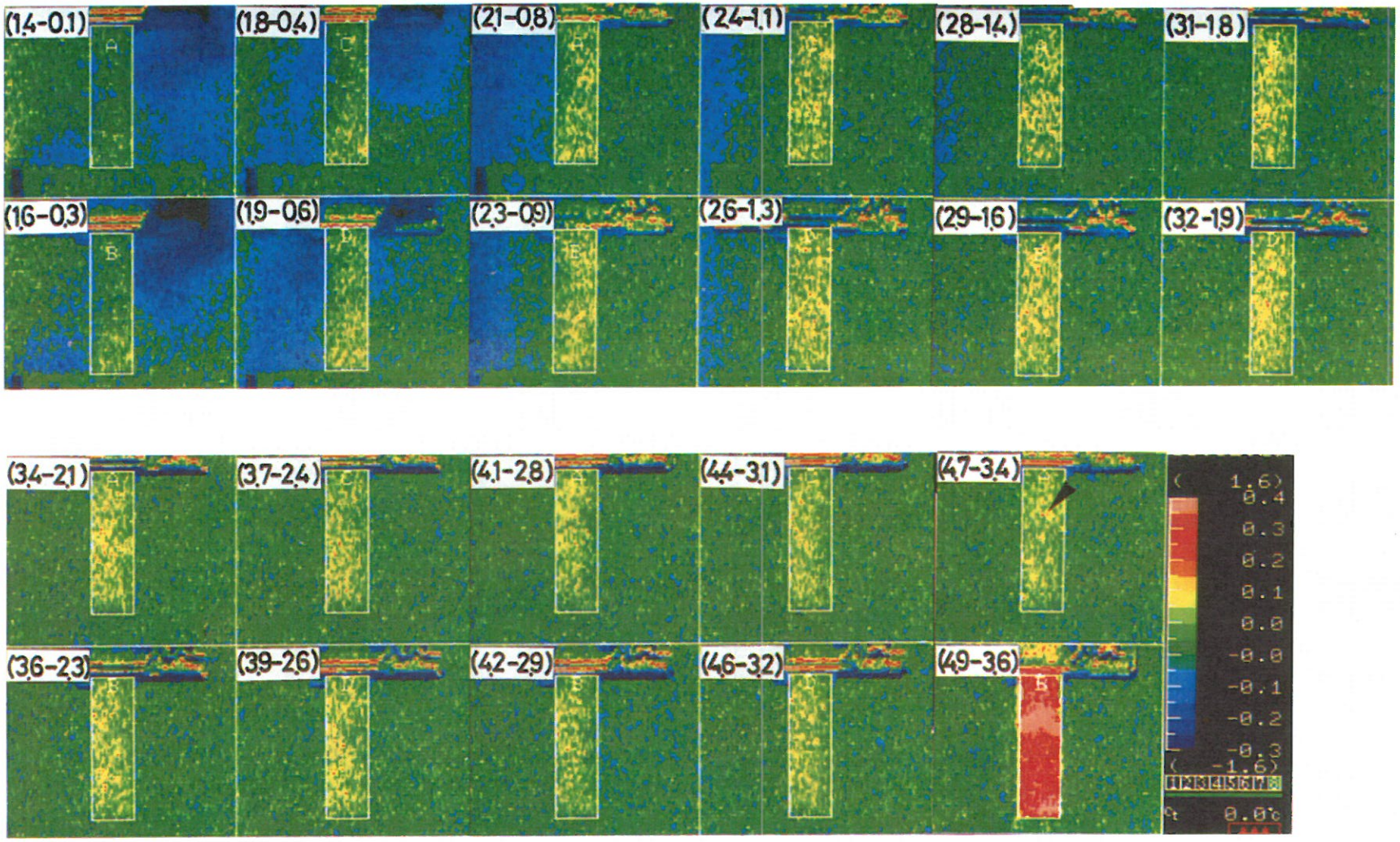

Fig 4b Sequential subtracted temperature images during straining for the handsheet made with bonding agent. Number in parentheses is percent elongation

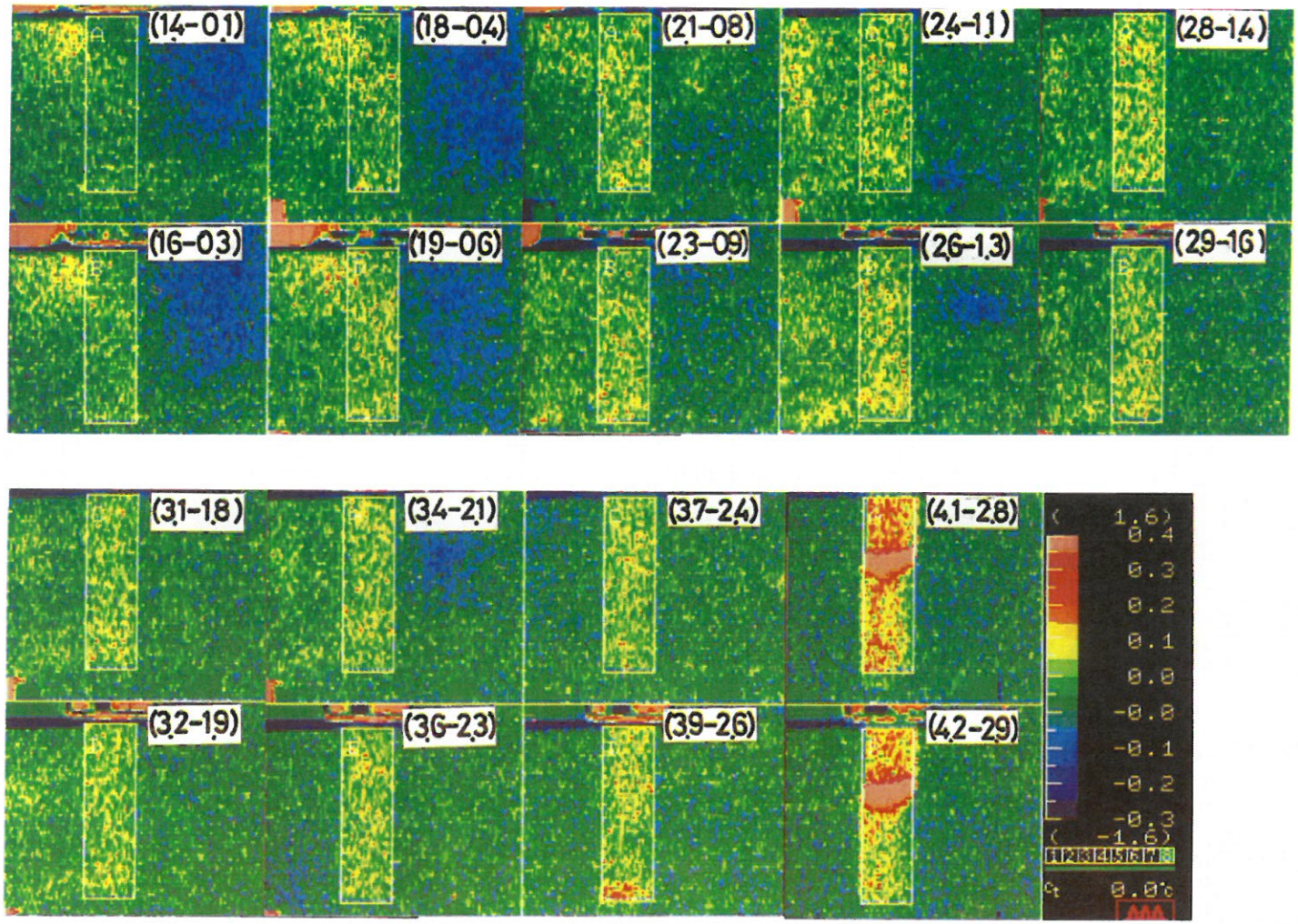

Fig 4c Sequential subtracted temperature images during straining for the control handsheet. Number in parentheses is percent elongation

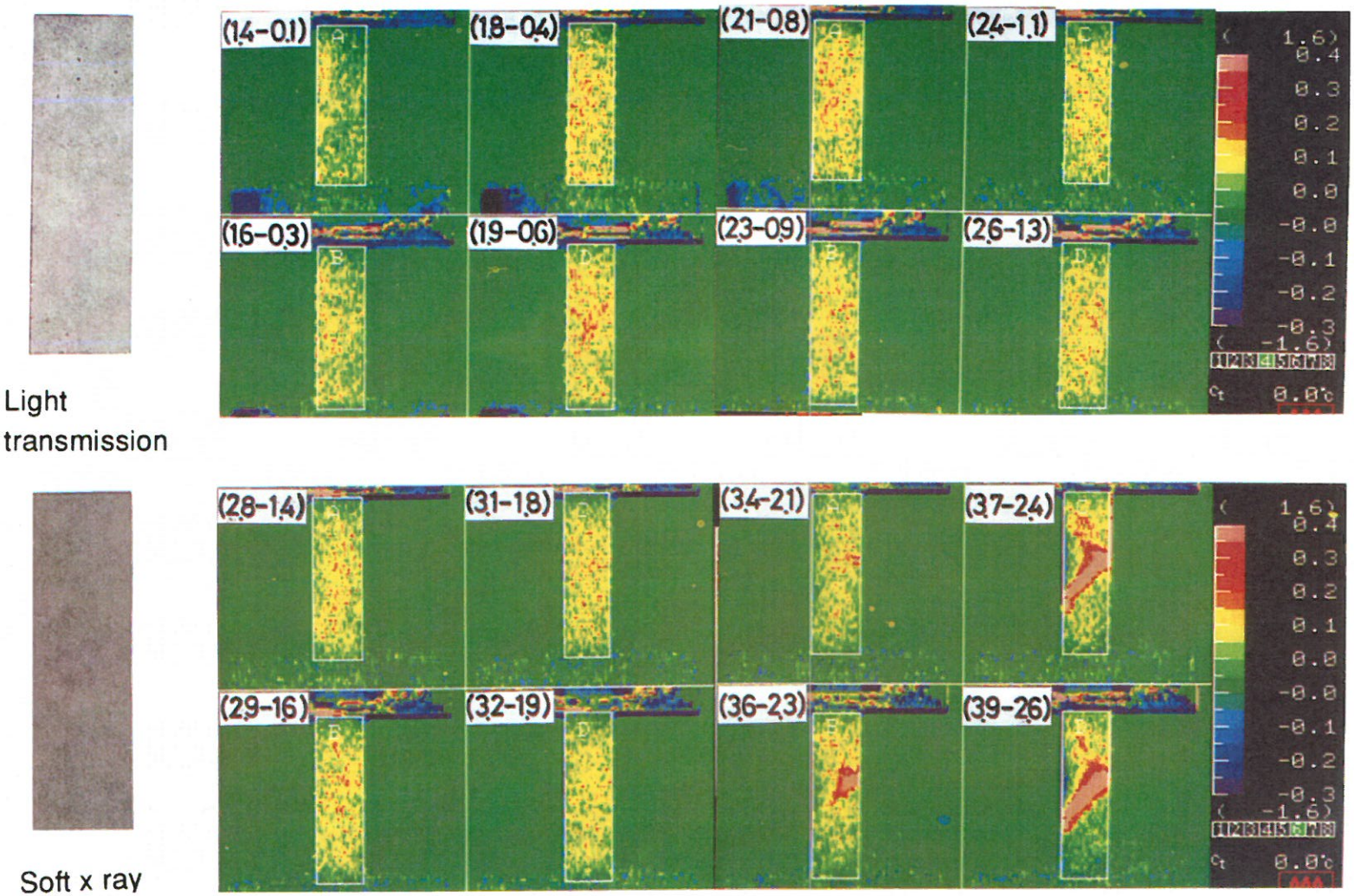

Fig 6a Light transmission and soft x ray images and sequential subtracted temperature images during straining for the handsheet made at normal forming stock concentration. Number in parentheses is percent elongation

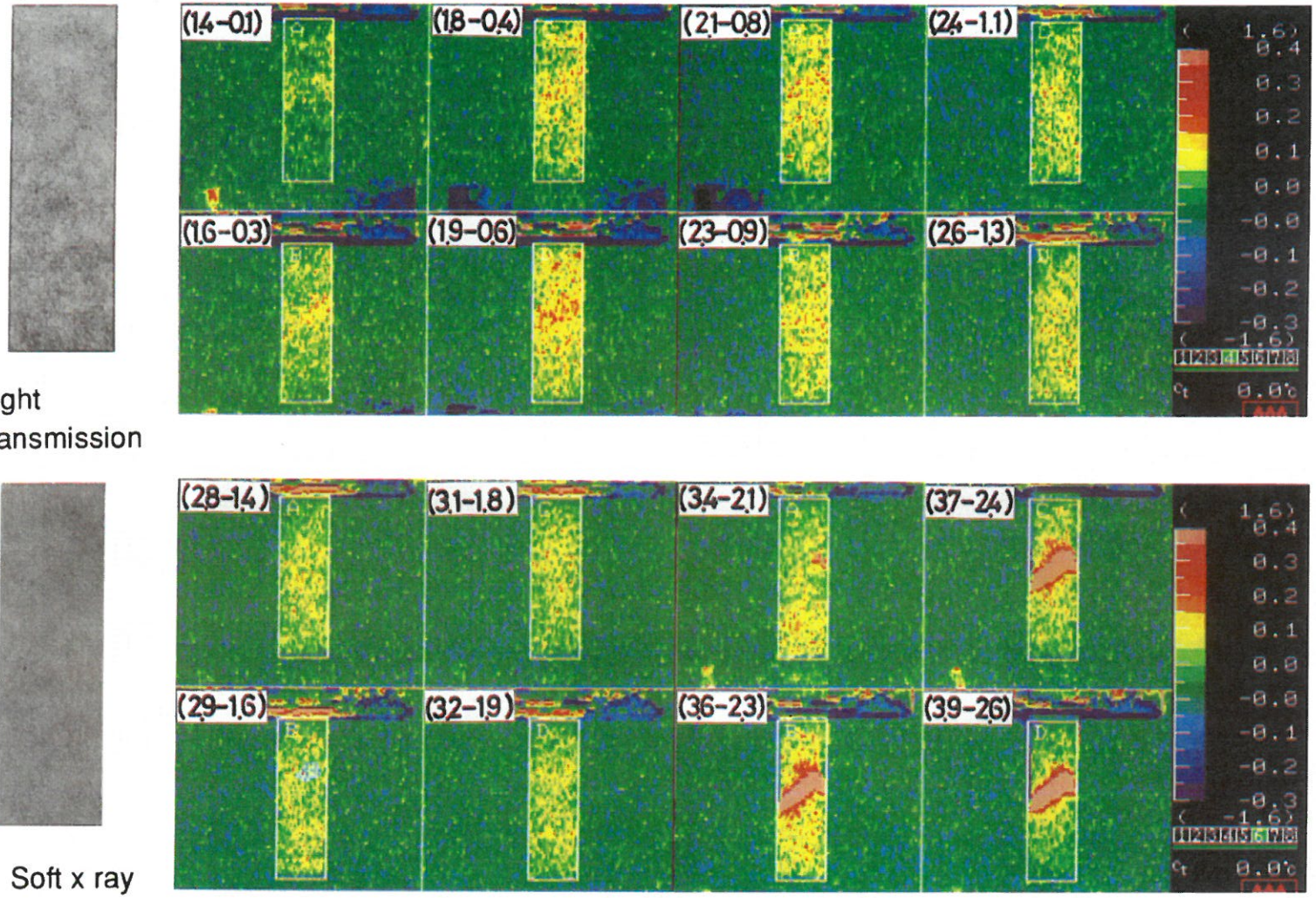

Fig 6b Light transmission and soft x ray images and sequential subtracted temperature images during straining for the handsheet made at 2 times thicker forming stock concentration. Number in parentheses is percent elongation

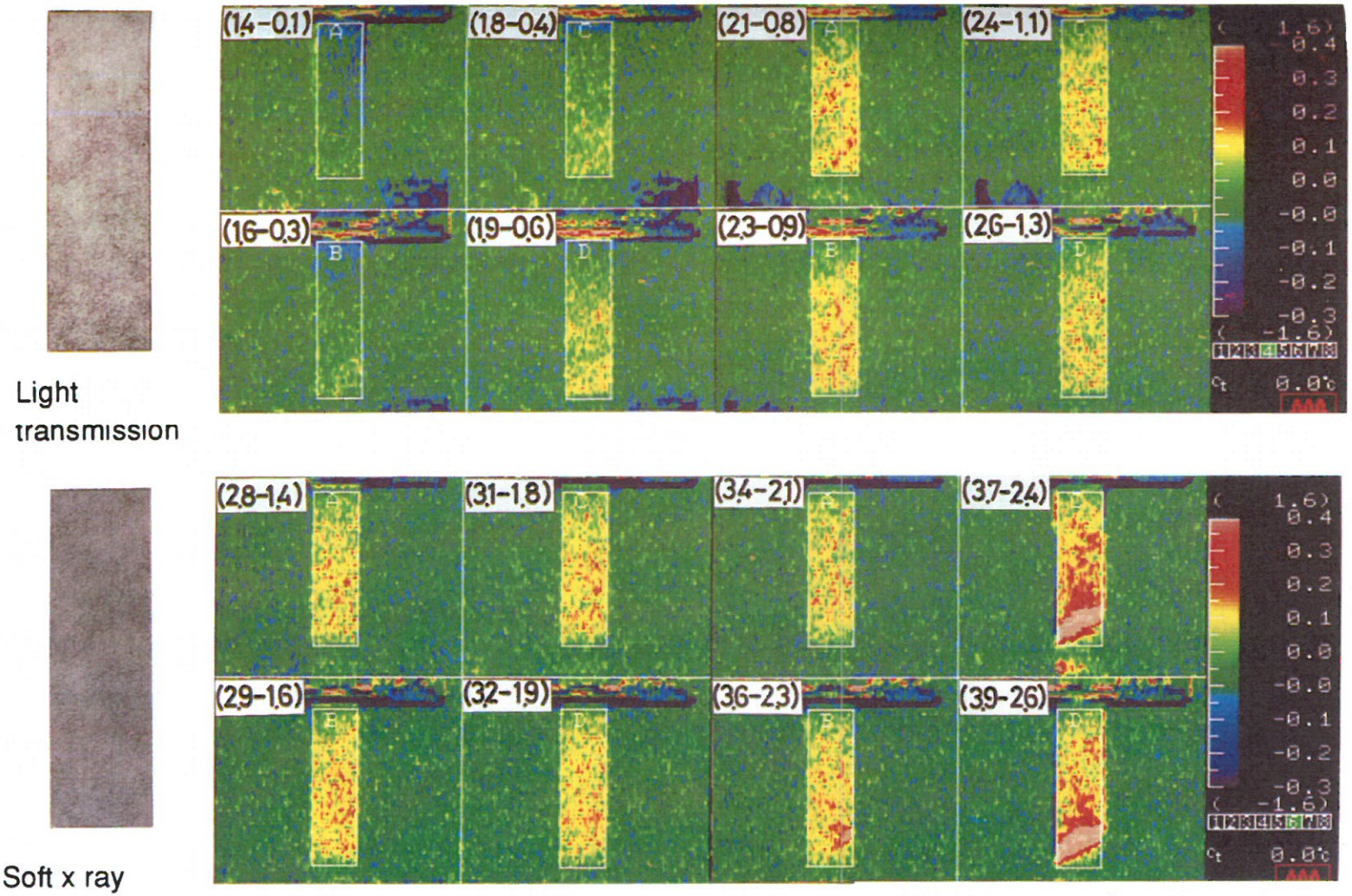

Fig 6c Light transmission and soft x ray images and sequential subtracted temperature images during straining for the handsheet made at 4 times thicker forming stock concentration. Number in parentheses is percent elongation

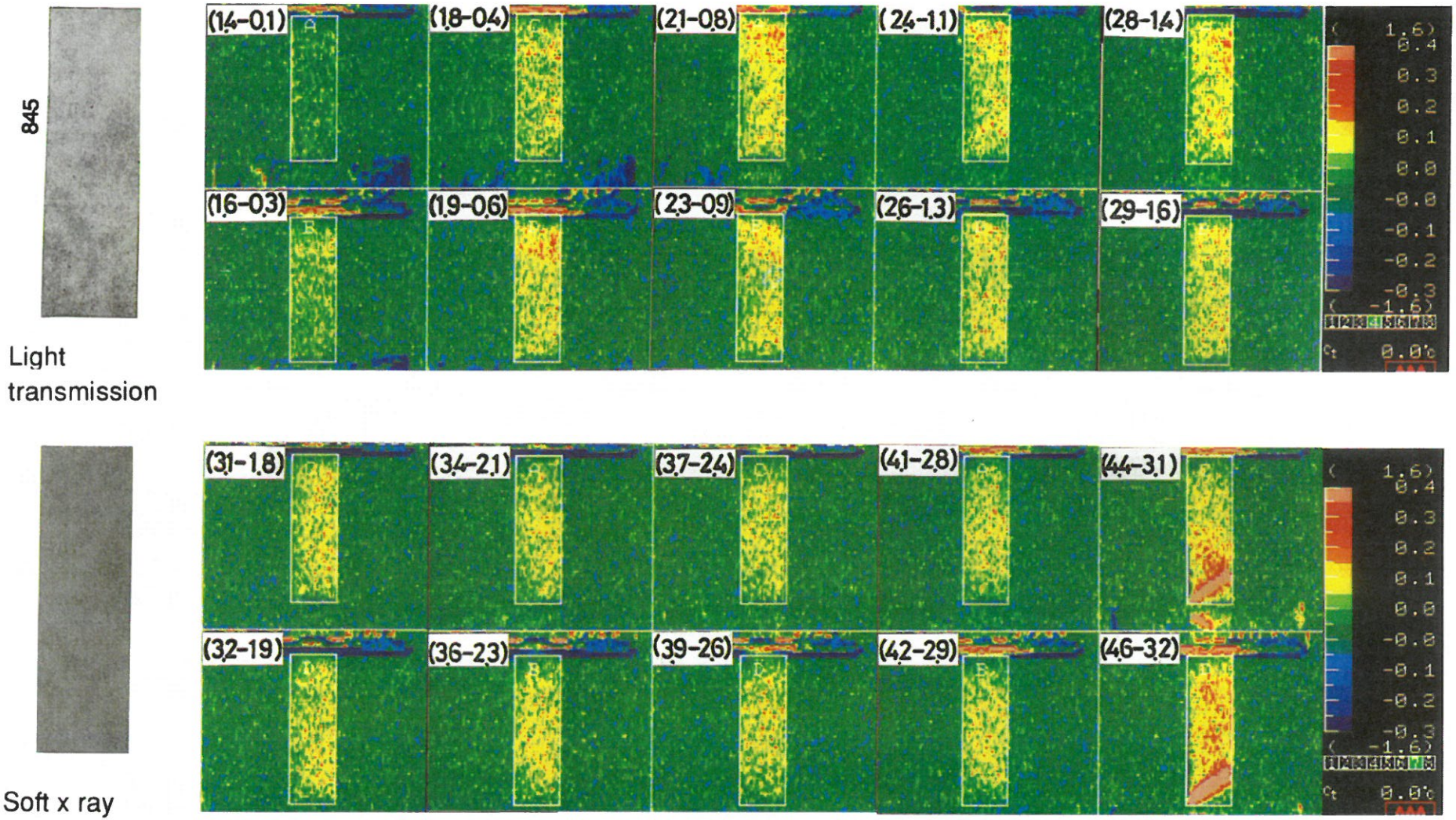

Fig 6d Light transmission and soft x ray images and sequential subtracted temperature images during straining for the handsheet made with 30 sec settling time. Number in parentheses is percent elongation

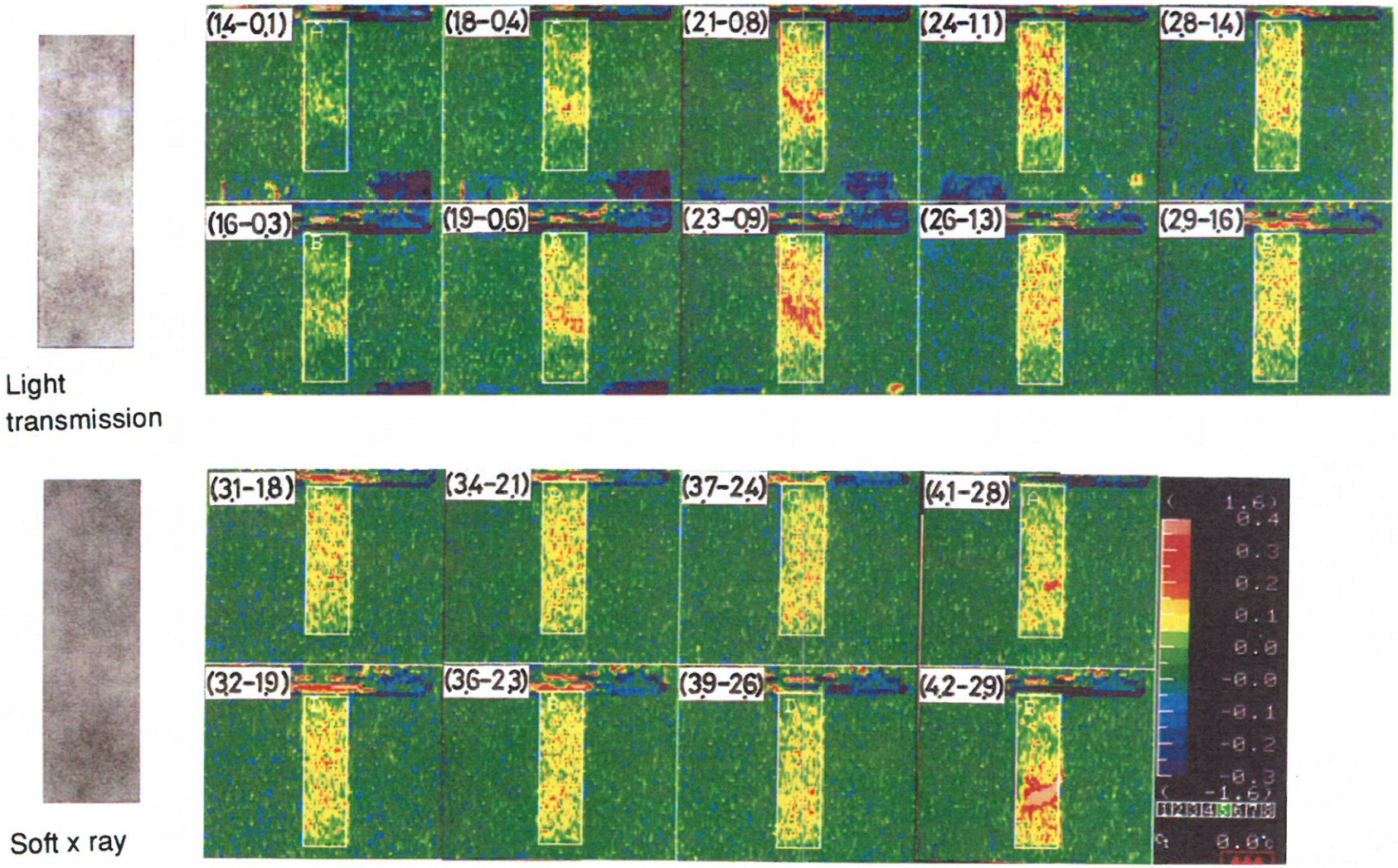

Fig 6e Light transmission and soft x ray images and sequential subtracted temperature images during straining for the handsheet made with 100 sec settling time. Number in parentheses is percent elongation

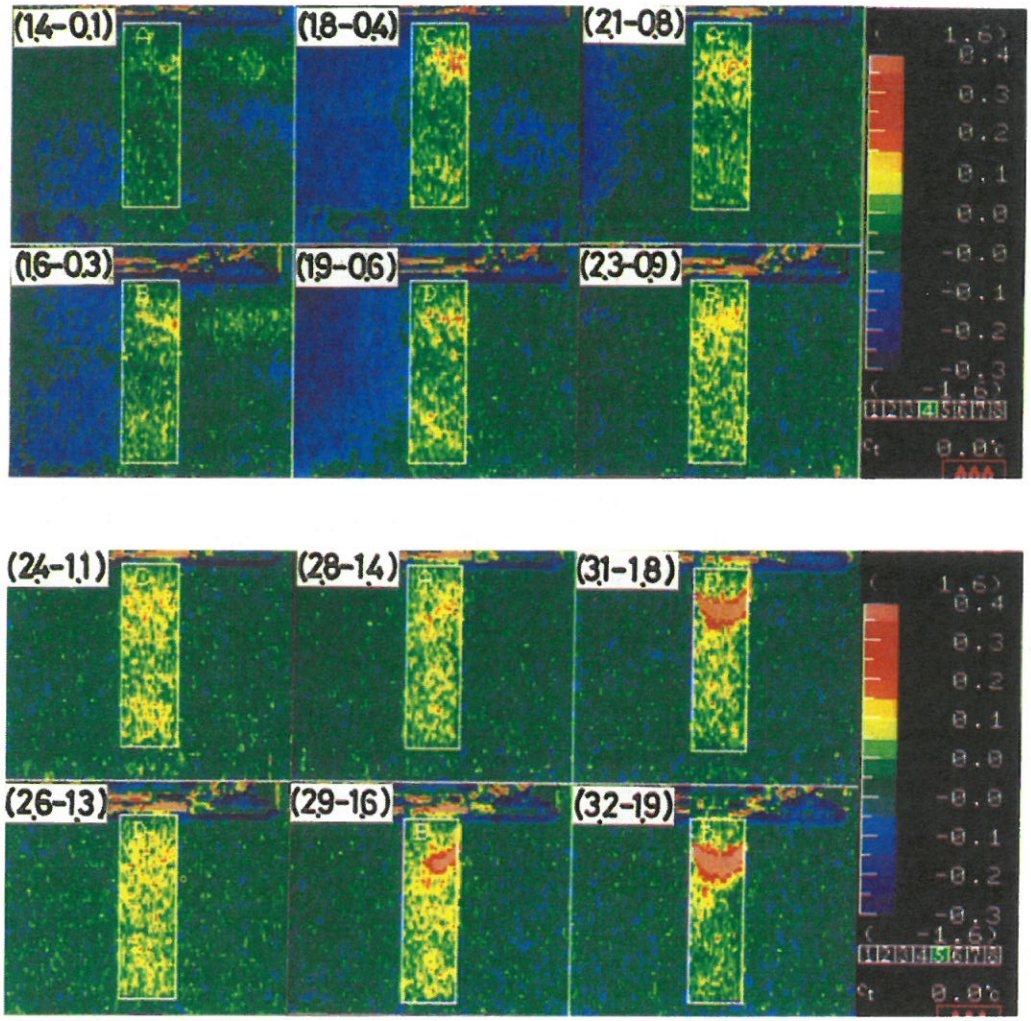

Fig 7 Sequential subtracted temperature images during straining for the combined sheet which is composed of a 50g/m^2 poorly formed handsheet and a 10g/m^2 well formed handsheet (top side). Number in parentheses is percent elongation

Transcription of Discussion

OBSERVATION OF DEFORMING AND FRACTURING PROCESS OF PAPER BY USING THERMOGRAPHY

T Yamauchi, K Murakami

ERRATA: At the bottom of page 832 Figure 4 should read Figure 6.

Prof C T J Dodson, University of Toronto, Canada
Two questions. The first is on the experimentation. Do you have the tables of data for the temperature and grammage of the samples or just the images?

T Yamauchi
Basis weight is the total only. I only measured the average.

C T J Dodson
Looking at the images one wonders whether you can answer Prof Kropholler's question, are poorly formed papers more tolerant of damage? From looking at the many examples you have studied, could you make a guess?

T Yamauchi
In the case of the poorly formed sheet, in the plastic deformation period paper justifies to get uniform load bearing I think and then the fairly uniform load bearing begins. This explanation is relating to the reason why the poorly formed sheet is lower on the strength.

Dr C Fellers, STFI, Sweden
We know that it would be a great advantage if we could detect cracks or flaws in a running web. Would it be possible to use this technique on a paper machine?

T Yamauchi
I think this condition is very severe. This method can only be used in the laboratory I think. Also I can just say that this is a fairly microscopic measurement now but with a different lens we can get a more magnified distribution image.

Dr G Baum, James River Corp, USA
How long does it take to make one scan?

T Yamauchi
In this case 0.25 sec.

P Herdman, Arjo Wiggins R&D Limited, UK
In the last month there has been some announcements about some charged coupled devices for making thermal images with exposure times of the order of a 10,000th of a second so it is possible to do this on moving webs now.

T Yamauchi
Yes, I have heard of this.